A STUDY ON TRANSVERSE VIBRATIONS IN A COLUMN AND AN OVERVIEW OF STRUCTURAL CONTROL

A Senior Scholars Thesis

by

ALEJANDRA LUCIA ROLDAN ARCOS

Submitted to the Office of Undergraduate Research
Texas A&M University
in partial fulfillment of the requirements for the designation as

UNDERGRADUATE RESEARCH SCHOLAR

July 2011

Major: Civil Engineering

A STUDY ON TRANSVERSE VIBRATIONS IN A COLUMN AND AN OVERVIEW OF STRUCTURAL CONTROL

A Senior Scholars Thesis

by

ALEJANDRA LUCIA ROLDAN ARCOS

Submitted to the Office of Undergraduate Research
Texas A&M University
in partial fulfillment of the requirements for the designation as

UNDERGRADUATE RESEARCH SCHOLAR

Approved by:

Research Advisor: Luciana Barroso
Director for Undergraduate Research: Sumana Datta

July 2011

Major: Civil Engineering

ABSTRACT

A Study on Transverse Vibrations in a Column and an Overview of Structural Control.
(July 2011)

Alejandra Lucia Roldan
Department of Civil Engineering
Texas A&M University

Research Advisor: Dr. Luciana Barroso
Department of Civil Engineering

During an earthquake, a building experiences seismic loads that may lead to the failure of structural members. In order to mitigate the dynamic loads, many are leaning heavily on structural control methods, which involve controlling the movement of the structure or of specific members to reduce the vibratory responses. It is vital to understand the behavior of the structural members experiencing the vibrations before being able to monitor and control them. Mode shapes show the different movement of columns by relying on the frequency the column experiences. These shapes can help to identify useful sensor locations. This research focuses on the structural characteristics of a column that experiences earthquake loads by (1) deriving transient vibrations with specific boundary conditions, (2) creating mode shapes to understand the movement of the column, and (3) providing location(s) for a structural control application using piezoelectric sensor(s). The paper will also give a background on the structural control that can be applied, and a proposed model for the column for further research.

DEDICATION

I would like to dedicate this work to Edwin S. Roldan. I looked up to you as my father and as an engineer. Thank you for encouraging the engineer side of me to grow throughout the years.

ACKNOWLEDGMENTS

I would like to express my gratitude Dr. Luciana Barroso for encouraging me to continue working and researching throughout the school year, especially during the most stressful parts of the research. Also, I would like to thank Dr. Stefan Hurlebaus with all of the transient equations and providing feedback on my work.

Thank you to the Undergraduate Research Scholars program, specifically Dr. Sumana Datta and Mrs. Tammis Sherman, for allowing me the opportunity to publish my thesis and my research work.

Additionally, I also would like to thank Mr. Benjamin Reid Dumas for Matlab debugging help and Mr. Douglas Simmons for moral support. Thank you also to Dr. Kohutek for steel design checks, and Dr. Lowery and Dr. Jones for helping me earn research credit.

NOMENCLATURE

MRD	Magneto-Rheological Damper
COC	Clipped-optimal control strategy
EMI	Electro-magnetic inductor
TMD	Tuned Mass Damper
P	Force
w	Transverse Displacement of the centerline of beam
$W_n(x)$	Mode Shape Equation
EoM	Equation of Motion
I.C.	Initial Condition(s)
B.C.	Boundary Condition(s)
ω	Frequency

TABLE OF CONTENTS

Page

ABSTRACT iii

DEDICATION iv

ACKNOWLEDGMENTS v

NOMENCLATURE vi

TABLE OF CONTENTS vii

LIST OF FIGURES ix

LIST OF TABLES xi

CHAPTER

I INTRODUCTION 1

Introduction to structural control 2
Magneto-rheological fluid damper 5
Introduction to piezoelectricity 8
Concept of vibration and mode shapes 10
Motivation and objectives 11

II METHODS 13

Overview: System simulation 13
Column background 14
Matlab program 20

III RESULTS 21

Transverse equation and mode shapes 21

IV CONCLUSION 24

REFERENCES 26

Page

APPENDIX EQUATION DERIVATIONS 29

Virtual work: Deflection shape 29
Transient equations and mode shapes 29
Data tables and figures 34
Matlab program 39

CONTACT INFORMATION 49

LIST OF FIGURES

FIGURE Page

1 Passive Flowchart....2

2 Structural (Active) Control System Flowchart....3

3 Structural (Semi-Active) Control System Flowchart....4

4 Magneto-Rheological Seismic Damper....5

5 Fluid Particles in MRD....6

6 (a) Direct and (b) Indirect Piezoelectric Effects....9

7 Superposition of Mode Shapes....11

8 The System with the Piezoelectric Strain Sensor and the Magneto-Rheological Damper Actuator....14

9 Column Model with Roller and Fixed Boundaries....15

10 Virtual Work Set-Up of Two Systems....16

11 (a),(b) Beam in Bending (Rao 2007)....17

12 Wide Flange Beam Cross Section....19

13 Column Mode Shapes....22

14 Plot of W_1', β_1....35

15 Plot of W_1'', β_1....36

16 Plot of W_1''', β_1....36

17 Plot of W_1^{IV}, β_1....37

18 Plot of W_2', β_2....37

19 Plot of W_2'', β_2....38

FIGURE Page

20 Plot of W_2''', β_2 38

21 Plot of W_2^{IV}, β_2 39

LIST OF TABLES

TABLE Page

1 Mode Numbers 21

2 Position of Maximum Curvature 23

3 The First Four Roots of $\tan\beta l = -\tanh\beta l$ 35

4 Dimensions of W12x87 Member Size 35

CHAPTER I

INTRODUCTION

In several parts of the world earthquakes can become a huge problem for civil engineers. Catastrophic outcomes occur after a city experiences strong seismic movements and plate shifting. For structural engineers the main focus in this case is keeping a structure standing, and minimizing the amount of displacement the structure experiences. This is vital in order to keep civilians safe and minimize the cost of repairs for structures.

This research focuses on the structural characteristics of a column that experiences earthquake loads by (1) applying transient vibrations specifically for the model boundary conditions, (2) creating mode shapes to understand the movement of the column, and (3) providing location(s) for a structural control application using piezoelectric sensor(s). The paper will also give a background on the structural control that can be applied, and a proposed model for the column for further research.

The research done allows a continuation for a more in depth analysis of the structural control impact of a Magneto-Rheological Damper system that is fed by a piezoelectric strain sensor placed at the maximum curvature position of a column experiencing transverse vibrations.

This thesis follows the style of *Journal of Intelligent Material Systems and Structures*.

Introduction to structural control

Strong earthquake excitations can lead to building collapses, bridge destructions, and can cause great risk towards civilian safety. Structural control is a means to mitigate the vibratory response of the structure subjected to natural or man-made excitations.

In order to control structures, structural dampers are introduced into buildings. The three classes of control devices are passive dampers, active dampers, and semi-active dampers (Bitaraf et al., 2010).

Passive control

A passive control system does not require an external power source to provide damping (Housner et al., 1997). The system uses the forces that are developed in the structure to control the motion of the structure. Examples of these kinds of dampers are Passive Fluid Viscous Dampers, Viscoelastic Dampers, Tuned Mass Dampers (TMD), and Tuned Liquid Dampers. *Figure 1* simplifies the functionality of a passive control system to show the vibratory excitation affecting the structure, allowing the structure to have a response.

Figure 1. *Passive Flowchart*

Active control

Active dampers are power driven to allow for a user to control the response of the structure by applying a force to it (Housner et al., 1997). These devices are adaptive to varying usage patterns and loading conditions but contain stability problems, require large power for workability (Bitaraf et al., 2010). Active control systems make use of actuators, such as active mass dampers and hybrid mass dampers (Housner et al., 1997). These dampers take advantage of the earthquake excitations by the use of smart sensors that help the damping system to provide a counter-response. There are two different types of control systems: feedback and feedforward control, as shown in *Figure 2*.

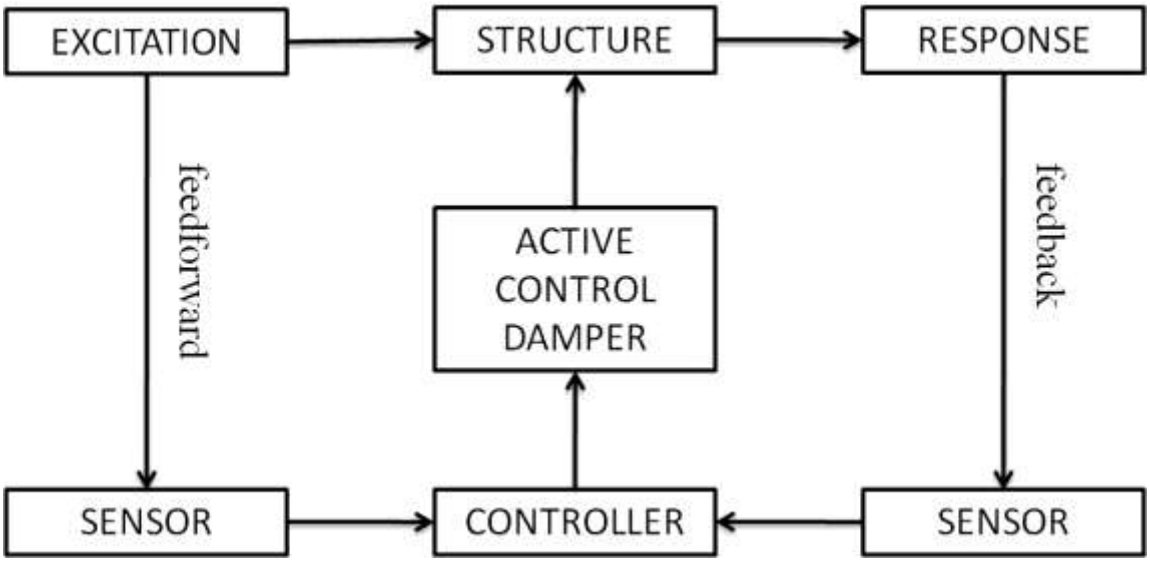

Figure 2. *Structural (Active) Control System Flowchart*

Semiactive control

Semiactive dampers act as an in-between passive and active damper, with some characteristics of both presented types of dampers. Semiactive dampers allow for control with a smaller magnitude of external power to be provided. In general most semiactive control devices do not add mechanical energy to the structure and therefore are more stable than active control systems (Housner et al., 1997). Semiactive control systems are also classified as controllable passive systems. Magneto-Rheological Dampers and Electro-Rheological Dampers have been an interest in the Smart Structures department due to their capability to adjust its properties from a passive to an active system. *Figure 3* shows an example of a semiactive system that includes a controller.

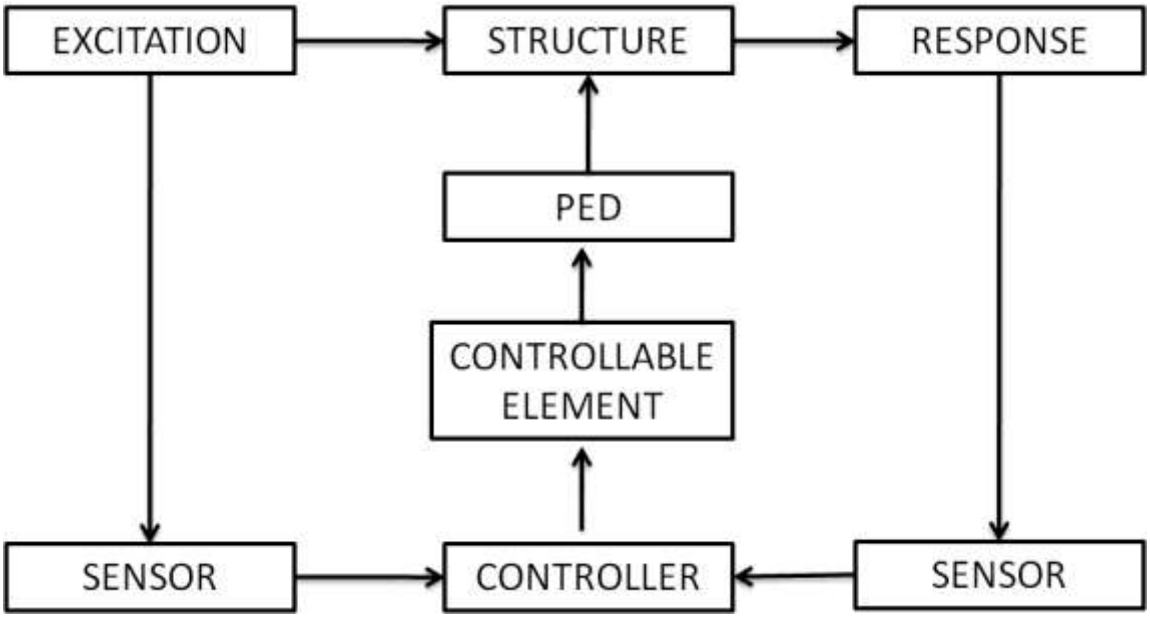

Figure 3. *Structural (Semi-Active) Control System Flowchart*

Magneto-rheological fluid damper

Magneto-Rheological Dampers (MRD) are a promising type of semi active control devices due to low power requirement to function while displaying almost the same damping characteristics as active systems (Bass and Christenson, 2007). Much research has been performed on the seismic response control of a structure implemented with MRD's. An example of an MRD manufactured by LORD Co. is shown in *Figure 4*.

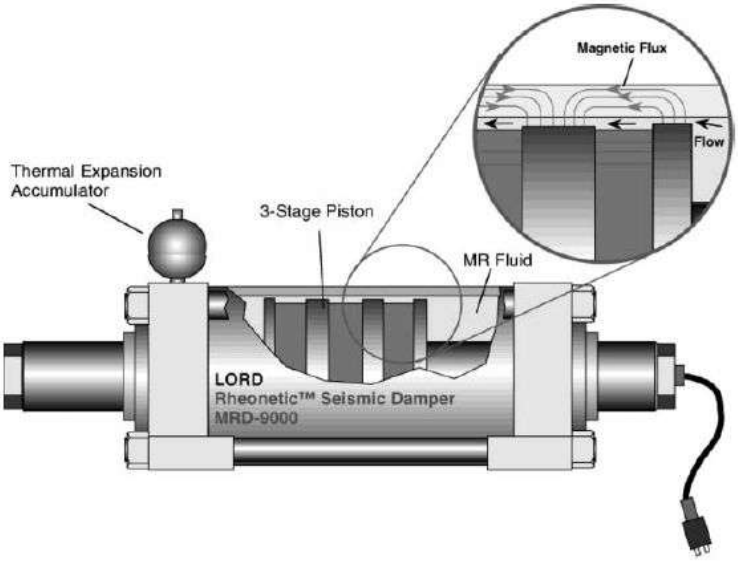

Figure 4. *Magneto-Rheological Seismic Damper*

MRD characteristics

The Magneto-Rheological Damper has the ability to reversibly change its rheological characteristics upon applying a magnetic field (Or et al., 2008). This is due to the Magneto-Rheological fluid particles that act like a free-flowing, low viscous fluid. The

particles line up and for a strong connection when a magnetic field is induced, changing the fluid to a semi-solid state with a controllable stress (Or et al., 2008) in real time. *Figure 5* shows the fluid particle transition from an initial state to a secondary stage after experiencing a current.

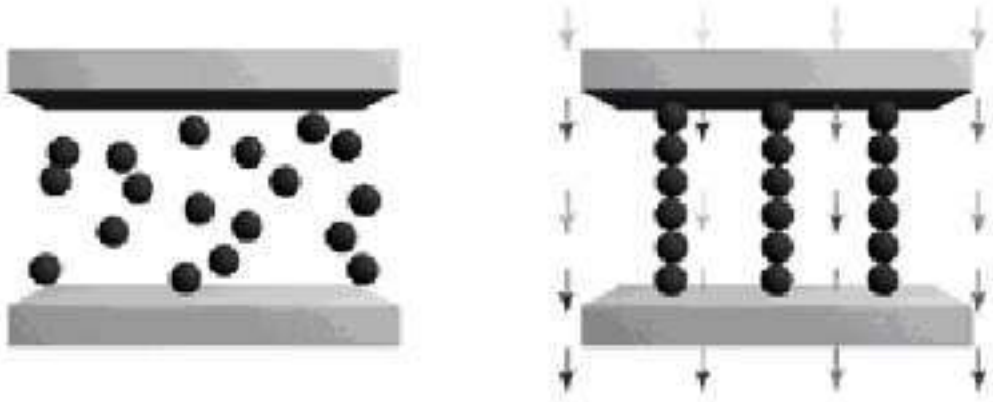

Figure 5. *Fluid Particles in MRD. (Left) Free-Flowing Fluid Particles Within MR Damper. (Right) Strong Connection Between the Particles After a Current is Applied to the MRD.*
(*http://www.brlsi.org/proceed05/postgrad0505.html)*

The MR damper provides great damping characteristics but it is dependent on another system supplying a current in order to damp. Therefore the MR damper is usually used with a primary controller that calculates the force desired for an effective damping on the system, which distributes the correct amount of current the MR fluid should experience. The current the MR damper experiences can be adjusted accordingly to provide a controllable damping force.

MRD models

It is hard to model the dynamics of the MR damper because of its inherent nonlinear behavior due to the highly viscous liquid when induced in a magnetic field. There are two types of dynamic models: parametric and non-parametric models. The nonparametric models are intelligent systems, such as the neural network-based models (Ni et al., 2002 and Xu et al., 2003), fuzzy logic-based models (Kim and Clark, 1999). The parametric models used to capture the MR damper behavior are the Bingham model (Lee and Wereley, 2002) and Bouc-Wen hysteresis model (Jansen and Dyke, 2000). Simulated research involves using different MRD models and adjusting the controllers that fed information to the MRD model. Dyke et al. (1996) developed the clipped-optimal control strategy (COC) model, Spencer et al. (1997) proposed the use of a phenomenological model based on the Bouc-Wen nonlinear element, while Bass and Christenson (2007) have worked on a Hyperbolic Tangent Model for a 200kN MR Fluid Damper. The MR damper has been used in conjunction with other systems. Jung et al. (2008) connected an EMI system that could send a current signal.

Much research has been done on structural control with a Magneto-Rheological Damper and on an individual piezoelectric sensor. Or et al. (2008) attempted to combine both topics by attaching a piezoelectric sensor to an MRD in order to provide a self-sensing and self-damping controller system, although the system still requires external power. The purpose of this paper is to provide information to be used with a MR Fluid damper system which would consist of using the Simple Bouc-Wen Model (Spencer et al., 1997)

to control the structure performance. This model can predict the force-displacement and force-velocity behavior well (Bitaraf et al., 2010).

Introduction to piezoelectricity

Piezoelectricity is the charge accumulated in piezoelectric material when it experiences a mechanical deformation. The direct piezoelectric effect is present when a mechanical deformation of a piezoelectric material produces a proportional charge in the electric polarization of that material (Gautschi, 2002). Piezoelectricity, therefore, is a result of the piezoelectric effect.

The piezoelectric effect was first observed in tourmaline crystals in India and Ceylon. These crystals would attract surrounding particles when they were thrown in into hot ashes and repel them later. This electrical phenomenon was proven by Aepinus in 1756 (Gautschi, 2002) and was named “pyroelectricity” in 1824.

In the late 1880s the Curie brothers reported announced their direct piezoelectric effect discovery in the Academie des Sciences in Paris. Although they did not term piezoelectricity, they presented their findings with respect to crystal symmetry and the effects that were observed.

The direct piezoelectric effect was not used as transduction elements in sensors to measure pressure, vibration, and forces until after WWI (Gautschi, 2002). *Figure 6* shows the direct and indirect piezoelectric effects.

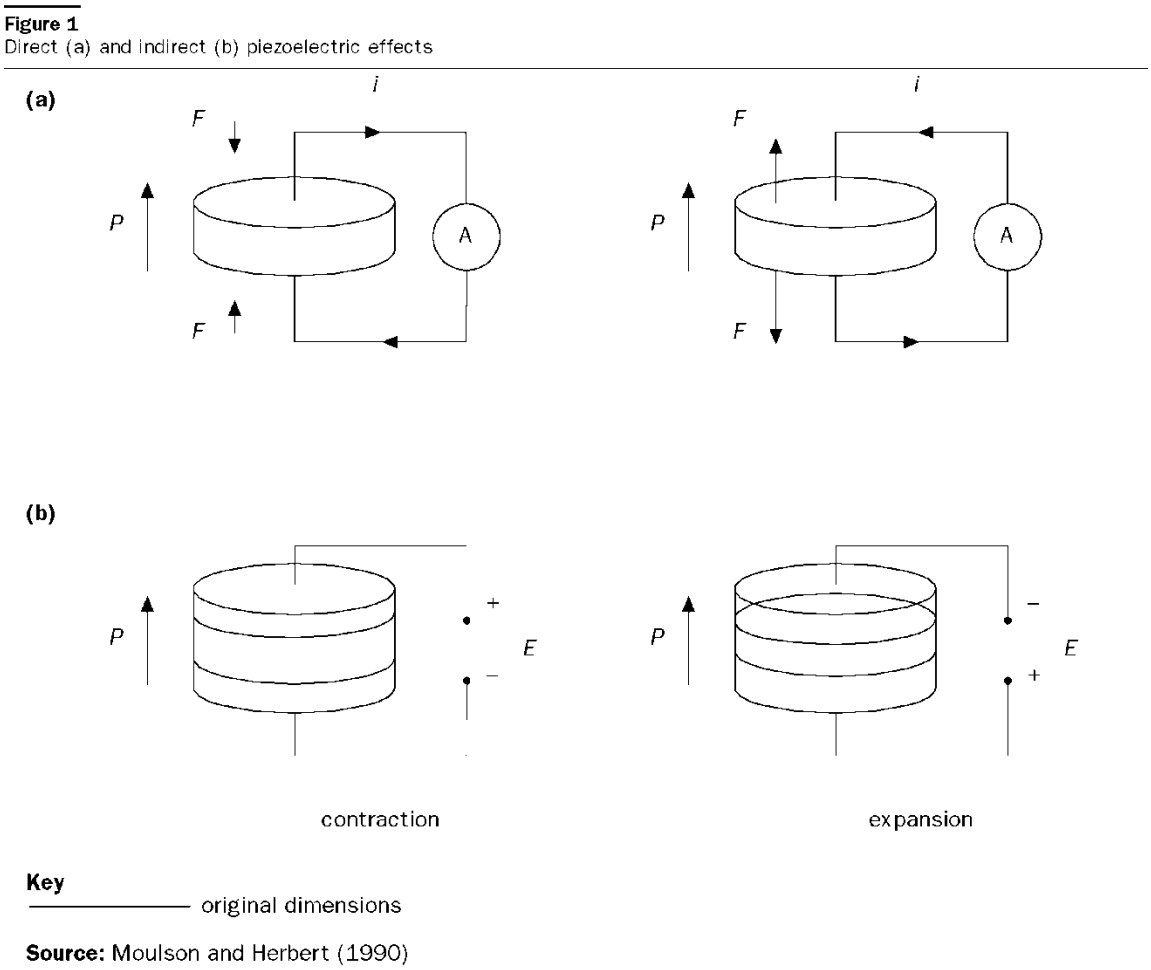

Figure 6. *(a) Direct and (b) Indirect Piezoelectric Effects*

A piezoelectric sensor is a device that uses the piezoelectric effect to measure pressure, acceleration, strain, or force (Piezocryst 2005). In this study, a column is induced with earthquake vibrations which allow it to experience sinusoidal movements. If a piezoelectric strain sensor is added to the maximum curvature location of the column, then the sensor can pass on clear strain readings to a semi-active system like the MRD.

Concept of vibration and mode shapes

According to Rao, any repetitive motion is called *vibration* or *oscillation* (Rao 2007). The initial excitation to a vibrating system can be in the form of initial displacement and/or initial velocity of the mass element(s) (Rao 2007). The initial excitation sets the system into oscillatory motion, which can be called *free vibration* (Rao 2007). If the system is given only an initial excitation, the resulting oscillatory motion eventually will come to rest for all practical systems, and hence the initial excitation is called *transient excitation* and the resulting motion is called *transient motion* (Rao 2007). A column experiencing an earthquake can be simply modeled by applying transient excitations, which this paper focuses on.

The phenomenon of mode shapes during the vibration of stretched strings, involving no motion at certain points and violent motion at intermediate points, was observed independently by Sauveur in France and John Wallis in England (Rao 2007). *Nodes* specified points with no motion, and *loops* were points with violent motion (Rao 2007).

When working with mode shapes, superposition—or adding together two or more systems—is used to model a system to its proximity. *Figure 7* shows this concept. Using basic mathematic theory, this method can also be used to scale the individual mode shapes and adding both of them together to obtain the final result that has also been scaled by a different factor.

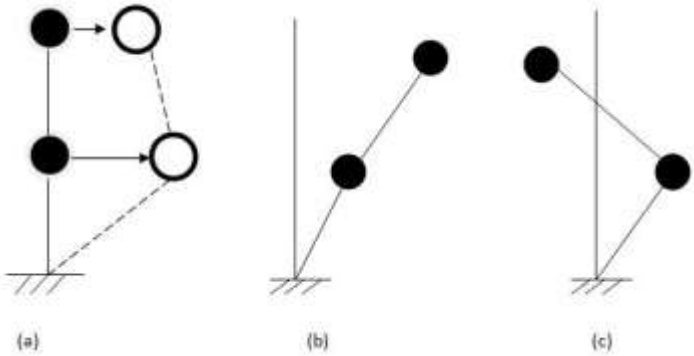

Figure 7. *Superposition of Mode Shapes. The movement of a Structure Can Be Modeled By Adding Two or More Equations or Mode Shapes. In This Case, (a) is the Summation of (b) and (c).*

Motivation and objectives

A detailed introduction to structural control and piezoelectricity has been presented in the previous sections to provide the reader a knowledgeable background on the current research topic. The information given also allows the reader to understand the final proposed model for further research with the current findings. This research focuses on the structural characteristics of a column that experiences earthquake loads by (1) applying transient vibrations specifically for the model boundary conditions, (2) creating

mode shapes to understand the movement of the column, and (3) providing location(s) for a structural control application using piezoelectric sensor(s).

CHAPTER II

METHODS

This section presents a brief overview of the theory used to derive important equations needed for the computer program, and implementation presented in the study.

Overview: System simulation

This study focuses on a column's characteristics when induced with earthquake loads.

Further research

The research provided is part of a more complex system that aims to control the column studied by using structural control. This study focuses on the structural control of a column using a piezoelectric strain sensor in order to feed information to a Magneto-Rheological Damper. An overview of the whole research is shown in *Figure 8.*

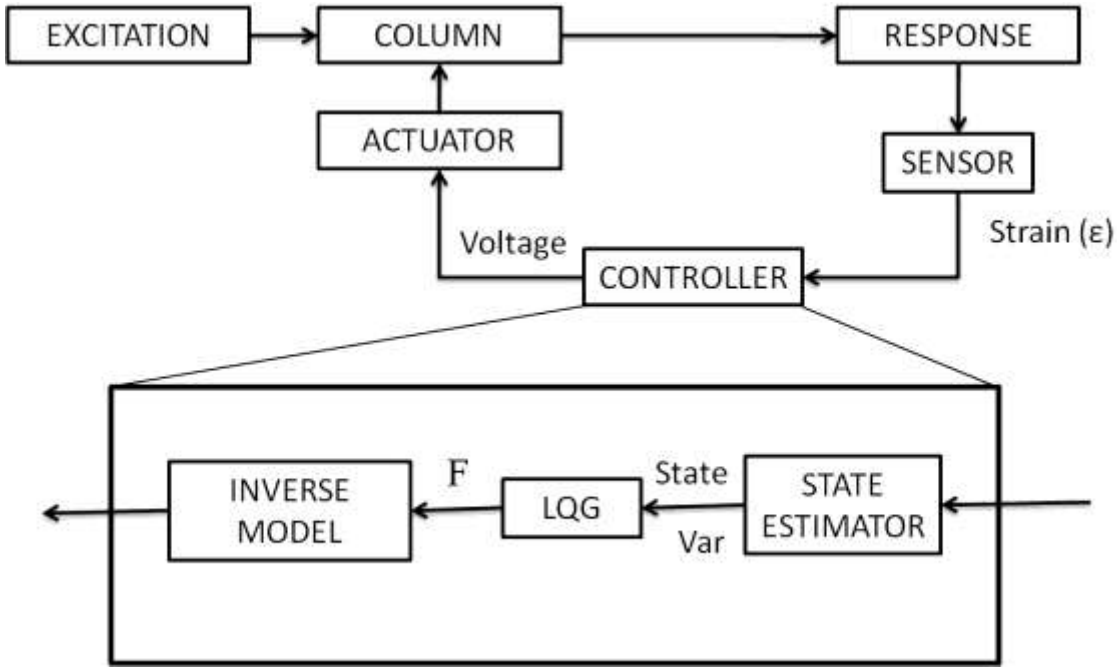

Figure 8. *The System with the Piezoelectric Strain Sensor and the Magneto-Rheological Damper Actuator*

In order to place the piezoelectric strain sensor in a location where it will be most convenient to the system, the curvature equation for the column is derived to find the maximum curvature location. The analytical model of the piezoelectric strain sensor uses the strain equation of the column, which is derived using unique boundary conditions in a transverse vibration equation.

Column background

This section gives an overview of the type of column used for analytical purposes and the different methods applied to analyze the column's characteristics.

Equation of columns

The column is modeled with a rigid support at the bottom and a roller at the top, as shown in *Figure 9*. The roller experiences a force P due to the seismic movement. The roller allows translation in the x-direction, but it also resists the column from curving at the wall connection.

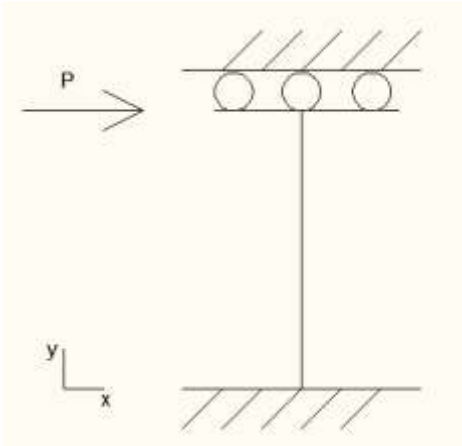

Figure 9. *Column Model with Roller and Fixed Boundaries*

The column model presented has three reactions at the fixed end and two reactions at the roller end, assuming the force P is known.

Virtual work is a procedure for computing a single component of deflection, or angle, at any point in a structure (Leet et al., 2008). This method works by superposition, meaning that two or more individual systems added together result in the real system. *Figure 10* shows the two systems used to derive the deflection equation for the column.

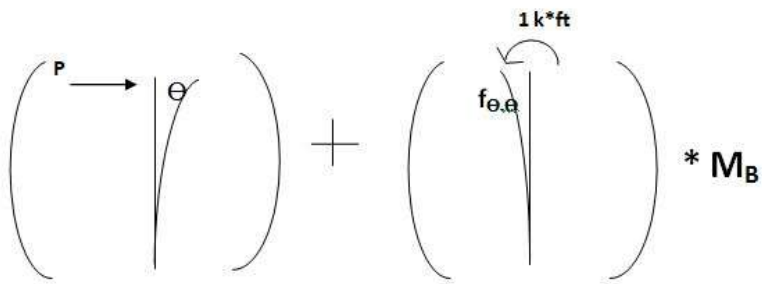

Figure 10. *Virtual Work Set-Up of Two Systems.System I (left) Shows the Deflection of the Column Due to an Applied Axial Force. System II (right) Models the Column Experiencing a CCW 1 k*ft Moment and Being Scaled by an M_B Moment.*

The compatibility equation of this system is shown in Equation 1.

$$0 = \theta + f_{\theta,\theta} * M_B \tag{1}$$

In order to derive the column's curvature equation a mechanics of materials equation is introduced.

$$\frac{d^2y}{dx^2} = \frac{M(x)}{EI(x)} \tag{2}$$

Equation 3 is derived using Equation 1 and Equation 2.

$$\frac{d^2y}{dx^2} = -\frac{Px}{EI} + \frac{PL}{2EI} \tag{3}$$

This equation, when integrated twice and using assumed boundary conditions, result in the column movement equation. This equation is used in the transient equation.

$$y(x) = -\frac{P}{EI}\left(\frac{x^3}{6} - \frac{x^2}{4}L\right) \tag{4}$$

Transverse vibrations using specific boundary conditions

The transverse vibrations of a beam rely on the equation of motion and boundary conditions of a beam. The thin beam theory is applicable to beams for which the length

is much larger than the depth and the deflections are smaller compared to the depth (Rao 2007). This thin beam theory is derived from *Figure 11*, which is shown below.

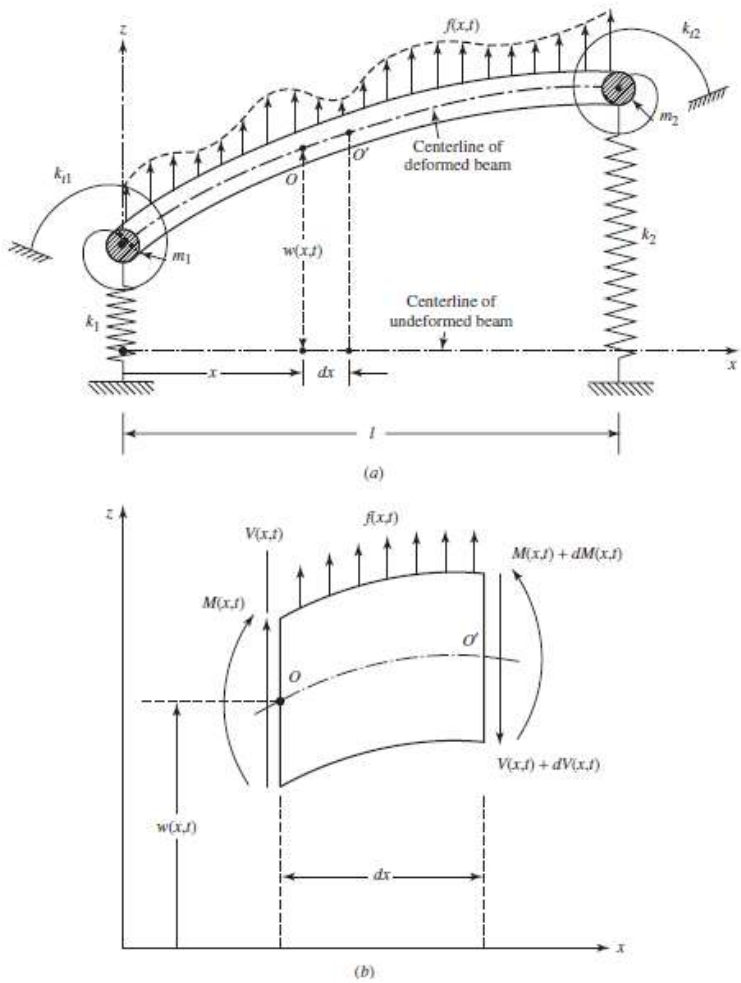

Figure 11. *(a),(b) Beam in Bending (Rao 2007)*

The variable w is the transverse displacement of the centerline of the beam.

The column model has a fixed end and a sliding ends. The fixed end has a zero deflection and a zero slope. The boundary conditions for the fixed end are shown in Equations 5 and 6.

$$w(l,t) = 0 \tag{5}$$

$$\frac{\partial w}{\partial x}(l,t) = 0 \tag{6}$$

The sliding end has a zero slope and a zero shear force. The boundary conditions for the sliding end are shown in Equations 7 and 8.

$$\frac{\partial}{\partial x}(0,t) = 0 \tag{7}$$

$$\frac{\partial}{\partial x}\left(EI\frac{\partial^2 w}{\partial x^2}\right)\bigg|_{0,t} = 0 \tag{8}$$

For the purpose of this analysis the column is treated as a horizontal beam. The equation of motion of a uniform beam in free vibration, accounting for the external vibrations equaling to zero, are shown in Equation 9 and 10.

$$c^2\frac{\partial^4 w}{\partial x^4}(x,t) + \frac{\partial^2 w}{\partial t^2}(x,t) = 0 \tag{9}$$

where

$$c = \sqrt{\frac{EI}{\rho A}} \tag{10}$$

The free vibrations solution of the column's equation of motion (*derived in Appendix A*) is shown in Equation 11 and 12.

$$T(t) = Acoswt + Bsinwt \tag{11}$$

$$W(x) = C_1(cos\beta x + cosh\beta x) + C_2(cos\beta x - cosh\beta x) + C_3(sin\beta x + sinh\beta x) + C_4(sin\beta x - sinh\beta x) \quad (12)$$

Column shape

The column shape used for analytical purposes was a W12x87, as shown in *Figure 12* below. The calculations for this column size and the calculations for this column size are shown in Appendix A and B, respectively.

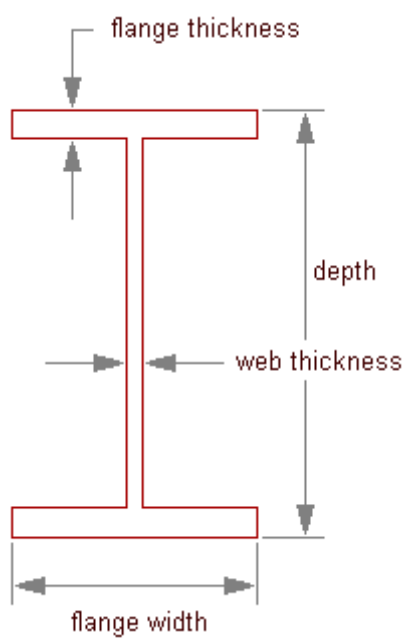

Figure 12. *Wide Flange Beam Cross Section. (AUTOCAD MEP, http://docs.autodesk.com)*

Matlab program

Different Matlab programs are created to analyze four different kinds of mode shapes for the column. *ModeFinding*, *MaxCurvature*, and *LocMaxCurv* are the user-defined functions that are within the main Matlab file *Checking_file* (See Appendix, A.4).

CHAPTER III

RESULTS

Transverse equation and mode shapes

The mode shape equation of the column, shown in Equation 13 and 14, are derived using the boundary conditions from Equations 4-7 with Equation 11.

$$W_n(x) = C_{4n}[(cos\beta_n x - cosh\beta_n x) + K_n(sin\beta_n x - sinh\beta_n x)] \tag{13}$$

$$K_n = \frac{sin\beta_n l + sinh\beta_n l}{cos\beta_n l - cosh\beta_n l} \tag{14}$$

The mode numbers for used in Equation 14 are equal to the roots of Equation 15.

$$\tan(\beta_n l) + \tanh(\beta_n l) = 0 \tag{15}$$

The roots for Equation 16, listed in Table 1, were used to derive the mode shapes and the dynamic characteristic of the column.

Table 1: Mode Numbers

$\boldsymbol{\beta_n l}$
2.3650
5.4978
8.6394
11.7810

Only the first four mode shapes were graphed, as shown in *Figure 13*, to explain the displacement and movement of the column.

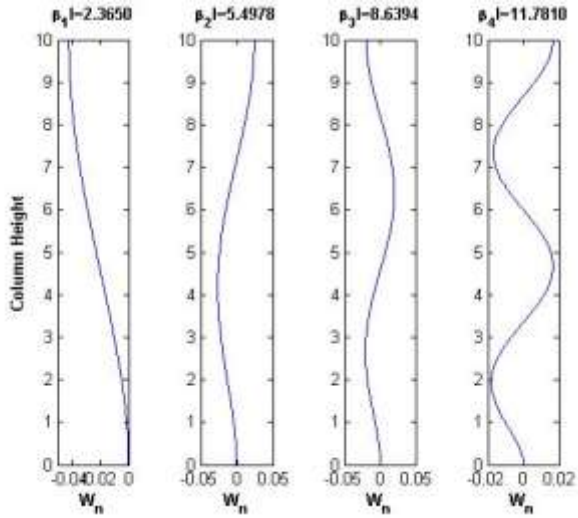

Figure 13. *Column Mode Shapes*

The curvature of the column equals the second derivative of the displacement of the beam equation. The location where the column experiences its maximum curvature was found by having the third derivative of $W_n(x)$ equal to zero.

$$W_n''' = C_{4n}\beta_n^3\,[\,(sin\beta_n x - sinh\beta_n x) \;+\; K_n(-cos\beta_n x - cosh\beta_n x)\,] \quad (16)$$
$$= 0$$

$$0 = \frac{\sin(\beta_n * x) - \sinh\,(\beta_n * x)}{\cos(\beta_n * x) + \cosh\,(\beta_n * x)} - K_n \quad (17)$$

The position of maximum curvature experienced by the column for each mode shape is shown on Table 2.

Table 2: Position of Maximum Curvature

Root	Max Curvature Position(s)
2.365	10
5.4978	4.4
	10
8.6397	2.8002
	6.3603
	10
11.781	2.0535
	4.6642
	7.3334

These positions were checked using the fourth derivative of $W_n(x)$, and by graphing the second and third derivatives, shown in Appendix. Two piezoelectric sensors should be placed at 4.4 and 6.4 feet upward from the bottom of the column.

In order to model the piezoelectric sensor, the relationship between the displacement of the member, in this case the column, and the strain it experiences shown in the following Equation 19 was used to obtain the analytical strain data.

$$\frac{du(x)}{dx} = \varepsilon(x) \tag{18}$$

$$\frac{dW_n(x)}{dx} = \varepsilon(x) \tag{19}$$

$$W_n(x) = C_{4n}[-(sin\beta_n x + cosh\beta_n x) + K_n(cos\beta_n x - sinh\beta_n x)] \tag{20}$$

CHAPTER IV

CONCLUSION

This project has been an important step in understanding the characteristics of a column, which will play a vital role in the structural control system introduced in the second section of Chapter II. The goals achieved in this research have been:

- Become knowledgeable of structural control
- Understand column characteristics
- Develop an equation for identifying column movement

Specifically, a transient equation that describes the movement of a column was derived, which allowed leeway to identify the location of the column's maximum curvature under an earthquake load represented by a transverse point load. Three new user-defined functions in the computer program Matlab were written and used successfully to create four mode shapes of the column by using the transient equation. Also, initial steps were taken in the area of identifying the normal mode equation of the column, which includes the transient equation derived.

An understanding of piezoelectricity, Magneto-Rheological Dampers, and structural control was documented for future reference in the next phases of the project. Given the

early stages of the research, there are many future improvements that can be made. The following bullet points propose important areas of improvement for future development.

- Improve variable callings in different Matlab user-defined functions, and provide a more user friendly program.
- Include forced vibration equation and compare to the current transient equation
- Check for other unit conflicts within the equations for strain equation derivation

The application of the above suggestions will likely enhance a closer relationship of the column model with a real-life column, which will be useful in the study of structural behavior.

REFERENCES

Bass, B.J and Christenson, R.E., 2007 "System Identification of a 200 kN Magneto-Rheological Fluid Damper for Structural Control in Large-Scale Smart Structures." *American Control Conference*. New York City.

Bitaraf, M., Ozbulut, O.E., Hurlebaus, S., and Barroso, L., 2010 "Application of Semi-Active Control Strategies for Seismic Protection of Buildings with MR Dampers." *Engineering Structures*, doi: 10.1016/j.engstruct.2010.05.023

Dyke, S.J., Spencer Jr., B.F., Sain, M.K., and Carlson, J.D., 1996 "Modeling and Control of Magnetorheological Dampers for Seismic Response Reduction." *Smart Materials and Structures*, 5(5), 565-575

Gautschi, G., 2002 *Piezoelectric Sensorics: Force, Strain, Pressure, Acceleration and Acoustic Emission Sensors, Materials and Amplifiers*. Springer-Verlag, Berlin Heidelberg.

Housner, G. W. , Bergman, L. A., Caughey, T. K., Chassiakos, A. G., Claus, R. O., Masri, S. F., Skelton, R. E., Soong, T. T., Spencer, B. F., and Yao, J. T. P., 1997 "Structural Control: Past, Present, and Future." *Journal of Engineering Mechanics*. 123(9), 897-971

Jansen, L.M. and Dyke, S.J., 2000. "Semiactive Control Strategies for MR Dampers: Comparative Study." *ASCE Journal of Engineering and Mechanics*, 126(8), 795-803.

Jung, H., Jang, D., and Lee, H., 2008 "Self Powered Smart Damping System Using MR

Damper." *15th International Congress on Sound and Vibration*, Daejeon, Korea.

Kim, S., and Clark, W. W., 1999 "Fuzzy Logic Semi-Active Vibration Control." *American Society of Mechanical Engineers, Aerospace Division (Publication) AD*, 59, 367-372

Lee, DY. and Wereley, N.M., 2002 "Analysis of Electro- and Magneto-Rheological Flow Mode Dampers Using Herschel-Bulkley Model." *SPIE Smart Structure and Materials Conference*, Newport Beach, CA.

Leet, K.M., Uang, C., and Gilbert, A., 2008 *Fundamentals of Structural Analysis* 3rd. McGraw-Hill, New York.

Ni, Y. Q., Liu, H. J., and Ko, J. M., 2002. "Experimental Investigation on Seismic Response Control of Adjacent Buildings Using Semi-Active MR Dampers." *SPIE- The International Society for Optical Engineering* 4696, 334-344

Or, S.W., Duan, Y. F., Ni, Y. Q., Chen, Z. H., and Lam, K. H., 2008 "Development of Magnetorheological Dampers with Embedded Piezoelectric Force Sensors for Structural Vibration Control." *Journal of Intelligent Material Systems and Structures*, 19(11), 1327-1338

Piezocryst Advanced Sensorics GMBH (2005). "Basics: Piezoelectric Sensors" <http://www.piezocryst.com/piezoelectric_sensors.php>

Rao, S.S., 2007 *Vibration of Continuous Systems.* John Wiley & Sons, New York

Spencer Jr., B.F. , Dyke, S.J., Sain, M.K., and Carlson, J.D. 1997. "Phenomenological Model for Magnetorheological Damper." *ASCE Journal of Engineering*

Mechanics Div. 123(3), 230-238

Xu, Z.-D., Shen, Y.P. and Guo, Y.-Q. 2003. "Semi-Active Control of Structures Incorporated With Magnetorheological Dampers Using Neural-Networks." *Smart Materials and Structures*, 12, 80-87.

APPENDIX

EQUATION DERIVATIONS

Virtual work: Deflection shape

This section shows the derivation of the deflection shape equation of a column with "fixed" and "sliding" boundary conditions using the Virtual Work method described in Chapter II.

$$\frac{d^2y}{dx^2} = -\frac{Px}{EI} + \frac{PL}{2EI} \tag{A.1.1}$$

Deriving the equation twice and keeping the constants in the equation give the following equation:

$$y(x) = -\frac{P}{EI}\frac{1}{6}x^3 + \frac{PL}{2EI}\frac{1}{2}x^2 + C_1x + C_2 \tag{A.1.2}$$

The boundary conditions used in this case are:

$$y(0) = 0 \tag{A.1.3}$$

$$y'(0) = 0 \tag{A.1.4}$$

Both boundary conditions given eliminate the constants and result in the following deflection shape equation:

$$y(x) = -\frac{P}{EI}\left(\frac{x^3}{6} - \frac{x^2}{4}L\right) \tag{A.1.5}$$

Transverse equations and mode shapes

The first part of the transient equation derivation is taken from the "Free Vibration Equation" section of Chapter 11 of *Vibration of Continuous Systems* (Rao 2007). The

final equation presented at the end is the equation specifically for the column in this paper.

Transient equation derivation

Since the external excitation for free vibrations is considered to be zero,

$$f(x,t) = 0 \tag{A.2.1}$$

And the Equation of Motion (EoM) becomes:

$$\frac{\partial^2}{\partial x^2}\left[EI(x)\frac{\partial^2 w(x,t)}{\partial x^2}\right] + \rho A(x)\frac{\partial^2 w(x,t)}{\partial t^2} = 0 \tag{A.2.2}$$

For a uniform beam, the EoM can be expressed as follows.

$$c^2\frac{\partial^4 w}{\partial x^4}(x,t) + \frac{\partial^2 w}{\partial t^2}(x,t) = 0 \tag{A.2.3}$$

where

$$c = \sqrt{\frac{EI}{\rho A}} \tag{A.2.4}$$

In order to solve for the free vibrations EoM, the method of separation of variables is used.

$$w(x,t) = W(x)T(t) \tag{A.2.5}$$

Rearranging the EoM using the equation above yields:

$$\frac{c^2}{W(x)}\frac{d^4W(x)}{dx^4} = -\frac{1}{T(t)}\frac{d^2T(t)}{dt^2} = a = \omega^2 \tag{A.2.6}$$

where $a = \omega^2$is a positive constant. The equation above can be rewritten as two equations:

$$\frac{d^4W(x)}{dx^4} - \beta^4 W(x) = 0 \tag{A.2.7}$$

$$\frac{d^2T(t)}{dt^2} + \omega^2 T(t) = 0 \tag{A.2.8}$$

where

$$\beta^4 = \frac{\omega^2}{c^2} = \frac{\rho A \omega^2}{EI} \tag{A.2.9}$$

The solution of the second of the two equations is given by

$$T(t) = Acos\omega t + Bsin\omega t \tag{A.2.10}$$

where A and B are constants that can be found from initial conditions. The solution to the first equation can be assumed to be of exponential form as

$$W(x) = Ce^{sx} \tag{A.2.11}$$

where C and s are constants. The auxiliary equation after substituting the solution to the equation becomes

$$s^4 - \beta^4 = 0 \tag{A.2.12}$$

The roots of the equation are given by

$$s_{1,2} = \pm\beta, \qquad s_{3,4} = \pm i\beta \tag{A.2.13}$$

The extended solution of the first equation is expressed as

$$W(x) = C_1 e^{\beta x} + C_2 e^{-\beta x} + C_3 e^{i\beta x} + C_4 e^{-e\beta x} \tag{A.2.14}$$

where $C_1, C_2,\ C_3$ and $C_4$are constants. The solution can be expressed with sines and cosines:

$$W(x) = C_1 cos\beta x + C_2 sin\beta x + C_3 cosh\beta x + C_4 sinh\beta x \tag{A.2.15}$$

or

$$W(x) = C_1(cos\beta x + cosh\beta x) + C_2(cos\beta x - cosh\beta x) + C_3(sin\beta x + sinh\beta x) + C_4(sin\beta x - sinh\beta x) \quad \text{(A.2.16)}$$

where $C_1, C_2,\ C_3$ and $C_4$are different constants for each case. The natural frequencies of the beam can be determined from Equation A.2.9 as:

$$\omega = \beta^2 \sqrt{\frac{EI}{\rho A}} = (\beta l)^2 \sqrt{\frac{EI}{\rho A l^4}} \quad \text{(A.2.17)}$$

The function $W(x)$ is known as the *normal mode* or *characteristic function* of the beam and ω is called the natural frequency of vibration. The value of β can be determined from the known boundary conditions of the beam.

Beam with applied boundary conditions

The column designed can be analyzed as a horizontal beam with a fixed and a sliding end. The boundary conditions for this case are as follows:

Left Boundary: Fixed End

$$w(0,t) = 0 \quad \text{(A.2.18)}$$

$$\frac{\partial w}{\partial x}(0,t) = 0 \quad \text{(A.2.19)}$$

Right Boundary: Sliding

$$\frac{\partial w}{\partial x}(l,t) = 0 \quad \text{(A.2.20)}$$

$$\frac{\partial}{\partial x}\left(EI\frac{\partial^2}{\partial x^2}\right)\bigg|_{(l,t)} = 0 \quad \text{(A.2.21)}$$

The normal mode function is rewritten as:

$$W(x) = C_1(cos\beta x + cosh\beta x) + C_2(cos\beta x - cosh\beta x) + C_3(sin\beta x + sinh\beta x) + C_4(sin\beta x - sinh\beta x) \quad \text{(A.2.22)}$$

I.C. –Left

$$0 = C_1(2) + C_2(1-1) \tag{A.2.23}$$

$$0 - C_3(2) + C_4(1-1) \tag{A.2.24}$$

Which yield

$$C_1 = C_3 = 0 \tag{A.2.25}$$

$$W(x) = C_2(cos\beta x - cosh\beta x) + C_4(sin\beta x - sinh\beta x) \tag{A.2.26}$$

I.C.-Right

$$\frac{\partial w}{\partial x} = C_2(-sin\beta l - sinh\beta l) + C_4(cos\beta l - cosh\beta l) = 0 \tag{A.2.27}$$

$$\frac{\partial^2 w}{\partial x^2} = C_2(-cos\beta l - cosh\beta l) + C_4(-sin\beta l - sinh\beta l) = 0 \tag{A.2.28}$$

$$\frac{\partial}{\partial x}\left(EI\ \frac{\partial^2 w}{\partial x^2}\right) = \frac{\partial}{\partial x} EI[-C_2(cos\beta l + cosh\beta l) - C_4(sin\beta l - sinh\beta l)] = 0 \tag{A.2.29}$$

$$= EI[C_2(sin\beta l - sinh\beta l) - C_4(cos\beta l + cosh\beta l)] = 0 \tag{A.2.30}$$

Applying to conditions to the $W(x)$ equation yields

$$-C_2(sin\beta l + sinh\beta l) + C_4(cos\beta l - cosh\beta l) = 0 \tag{A.2.31}$$

$$C_2(sin\beta l - sinh\beta l) - C_4(cos\beta l + cosh\beta l) = 0 \tag{A.2.32}$$

For a nontrivial solution of C_1 and C_4, the determinant of their coefficients must be zero:

$$\begin{vmatrix} -(sin\beta l + sinh\beta l) & cos\beta l - cosh\beta l \\ sin\beta l - sinh\beta l & -(cos\beta l + cosh\beta l) \end{vmatrix} = 0 \tag{A.2.33}$$

$$2sin\beta l cosh\beta l + 2sinh\beta l cos\beta l = 0 \tag{A.2.34}$$

$$tan\beta l = -tanh\beta l \tag{A.2.35}$$

The roots of this equation, $\beta_n l$, give the natural frequencies of vibration:

$$\omega_n = (\beta_n l)^2 \left(\frac{EI}{\rho A l^4}\right)^{\frac{1}{2}}, n = 1,2, \ldots \tag{A.2.36}$$

The value of C_4 corresponding to β_n is denoted as C_{4n}, it can be expressed in terms of C_{2n}:

$$C_{4n} = C_{2n} \frac{cos\beta_n l - cosh\beta_n l}{sin\beta_n l + sinh\beta_n l} \tag{A.2.37}$$

$$W_n(x) = C_{2n} \left[(sin\beta_n l - sinh\beta_n l) - \frac{cos\beta_n l - cosh\beta_n l}{sin\beta_n l + sinh\beta_n l} (cos\beta_n l + cosh\beta_n l) \right] \tag{A.2.38}$$

The first four roots of $tan\beta l = -tanh\beta l$ are shown in Table 3.

Data tables and figures

This section is dedicated to information that has not yet been introduced in the body of the paper. *Figure 14* through *Figure 21* are graphs of the second, third, and fourth derivative of $W_n(x)$ that show the root, or the location on the beam of the x-axis intersection. The second derivative shows the maximum curvature, which is checked with the root of the third derivative, and the sign of the fourth derivative. The first row of figures show the result for the first mode shape, or β_1. The second row of figures show the result for the second mode shape, or β_2.

Table 3. The First Four Roots of $\tan\beta l = -\tanh\beta l$

0.1571
0.2365
0.4712
0.5498

Table 4. Dimensions of W12x87 Member Size

W12x87		
Ag	25.6	in^2
Ix	740	in^4
rx	5.38	in
tw	0.515	in
bf	0.81	in
Iy	241	in^4
ry	3.07	In

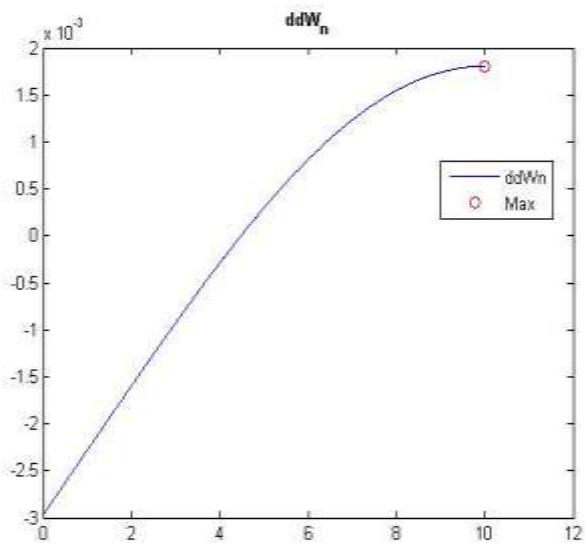

Figure 14.*Plot of* W_1', β_1

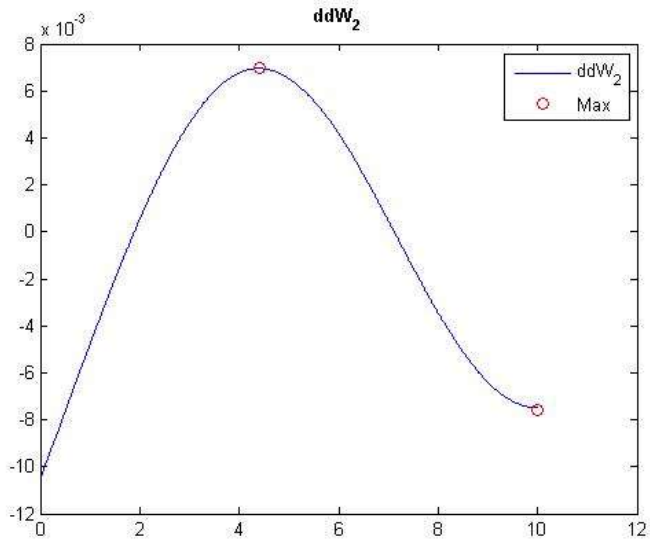

Figure 15. *Plot of* W_1'', β_1

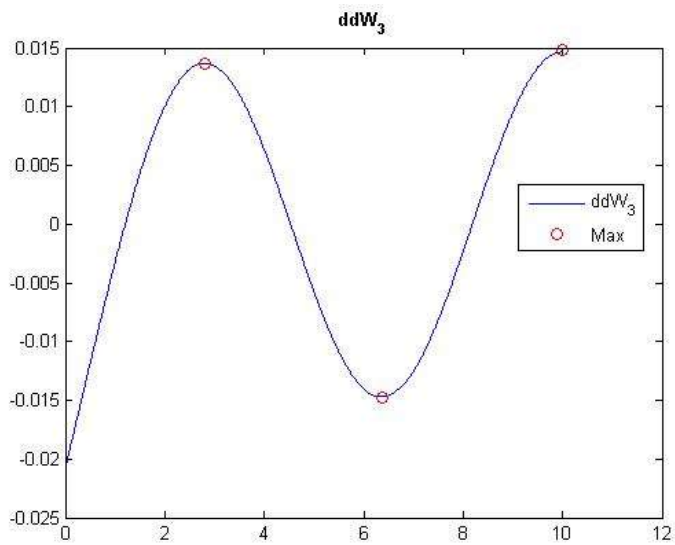

Figure 16. *Plot of* W_1''', β_1

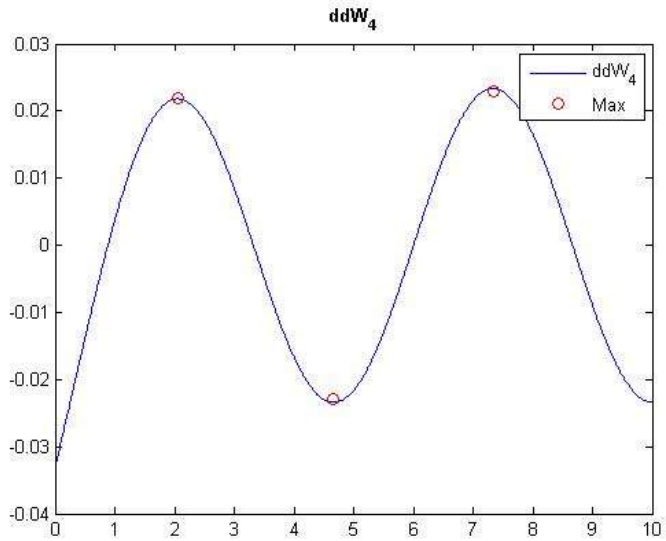

Figure 17. *Plot of* W_1^{IV}, β_1

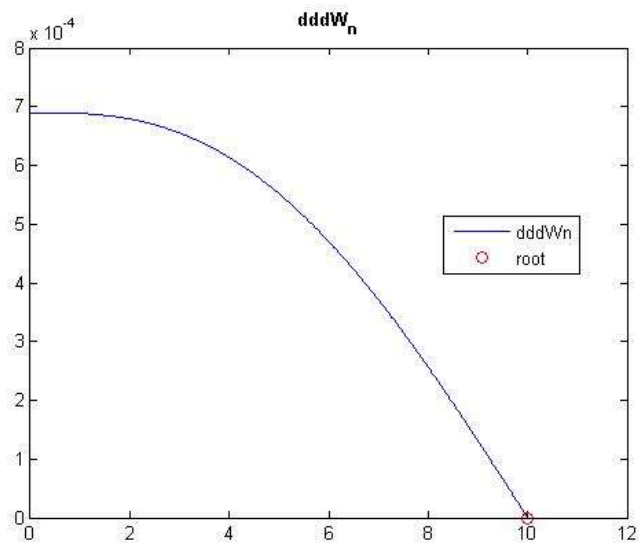

Figure 18. *Plot of* W_2', β_2

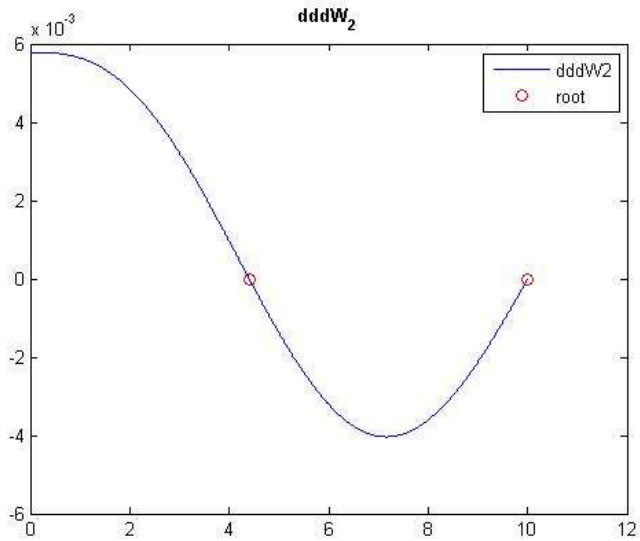

Figure 19. P*lot of* W_2'', β_2

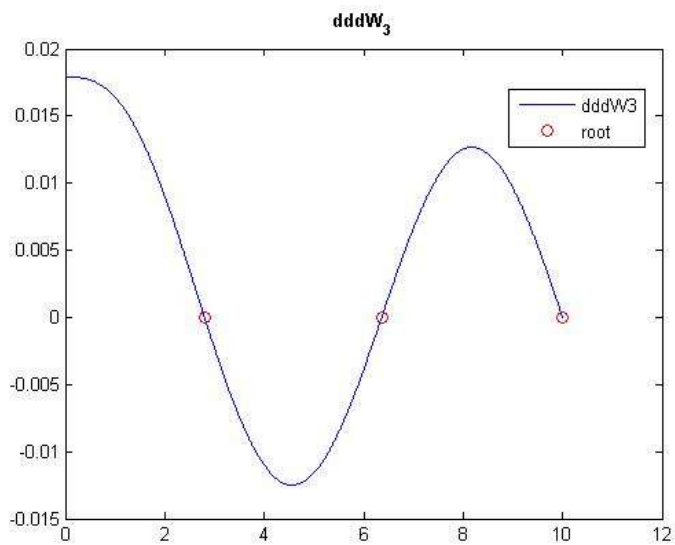

Figure 20. *Plot of* W_2''', β_2

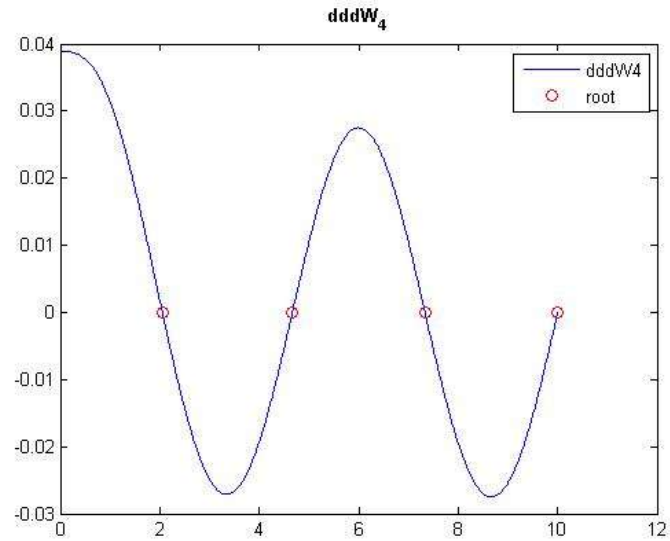

Figure 21. *Plot of* $W_2^{\mathrm{IV}}, \beta_2$

MATLAB program

Checking_file.m

This function is the main program that calls the other user defined functions.

```
clc;clear;clf;
%     ---------------------------------------------------     %
%                                                             %
%             Undergraduate Research Scholars                 %
%             Transient Equation with Mode Shapes             %
%                  Main Program (as of 3/23/11)               %
%
% Roldan, Alejandra L.
% Modified last: 3/23/11

global BETA l p A CONST C4

%....... Begin Code Block 1
ModeFinding;
%....... End of Code Block 1


% ................. Begin Code Block 2: Root 1
K=CONST(1);
B = BETA(1); % independent on defined length
C4n = C4(1);

f = @(y) (sin(y)-sinh(y))/((cos(y)+cosh(y)))-K;
```

```
y = fzero(f,1);
x = y/B;
% % Check:
zero=(sin(y)-sinh(y))/(K*(cos(y)+cosh(y)))-1;

z=0:0.01:1;
W1    = (C4n * B^0) .*( (cos(B.*z) - cosh(B.*z) ) + ...
             K .* (sin(B.*z) - sinh(B.*z)) );
dW1   = (C4n * B^1) .*( (-sin(B.*z) - sinh(B.*z) ) + ...
             K .* (cos(B.*z) - cosh(B.*z)) );
ddW1  = (C4n * B^2) .*( (-cos(B.*z) - cosh(B.*z) ) + ...
             K .* (-sin(B.*z) - sinh(B.*z)) );
dddW1 = (C4n * B^3) .*( ( sin(B.*z) - sinh(B.*z) ) + ...
             K .* (-cos(B.*z) - cosh(B.*z)) );
ddddW1= (C4n * B^4) .*( ( cos(B.*z) - cosh(B.*z) ) + ...
             K .* (sin(B.*z) - sinh(B.*z)) );

figure(2)
subplot(1,5,1)
plot(W1,z)
subplot(1,5,2)
plot(dW1,z)
subplot(1,5,3)
plot(ddW1,z)
subplot(1,5,4)
plot(dddW1,z)
hold on
plot(0,x,'ro')
% axis([0 0.001 0 10])
subplot(1,5,5)
plot(ddddW1,z)
hold on
plot(z,'r')

% plot settings
subplot(1,5,1); title('\bfW_1')
subplot(1,5,2); title('\bfdW_1')
subplot(1,5,3); title('\bfddW_1')
subplot(1,5,4); title('\bfdddW_1')
subplot(1,5,5); title('\bfddddW_1')
```

ModeFinding.m

This user defined function uses the transient equation $W_n(x)$ to locate the mode for the first four mode shapes.

```
function [] = ModeFinding ()
%                  Undergraduate Research Scholars
%                   Transient Equation with Mode Shapes
```

```
%
% Roldan, Alejandra L.
% Modified last: 3/23/11
%
% ==============================================================
% ||                        VARIABLES                          ||
% ==============================================================
%     C2                     Normalized constant
%     l                      length of column
%     BETA                   Modes calculated with defined Length
%     Wn                     normal mode or characteristic function
%     p                      density of column (*)
%     A                      Area of Column (*)
%     CONST                  Kn value from Wn equation
%
% ----------------  ** Useful defined Equations ** ----------------
%
%  (1)   W_n(x)  =  C_4n * ( cos Bx - cosh Bx ) + Kn * ( sin Bx - sinh
Bx )
%  (2)     Kn    =  ( sin B*l + sinh B*l ) / ( cos Bl - cosh Bl )
%
% ---------------- ---------------- ---------------- ----------------

global BETA l p A CONST C4 Wn ModVal1

l=10; % [ft]
x=0:0.01:l; %[ft]
p = 0.00881453392; % slugs / (in^3) = 7850 kg/m3 A992 Steel
% W 12x87 PROPERTIES
A = 25.6; % in^2
Ix = 740;Iy = 241; % in^4
rx = 5.38; ry = 3.07; % in.
tw = 0.515; % in.
bf = 0.810; % in.
% ------------------------------- ROOTS -------------------------------
 %
f = @(y) tan(y)+tanh(y);
 B(1,1) = fzero(f,3); B(1,2)=tan(B(1,1))-tanh(B(1,1));
 B(2,1) = fzero(f,6); B(2,2)=tan(B(2,1))-tanh(B(2,1));
 B(3,1) = fzero(f,9); B(3,2)=tan(B(3,1))-tanh(B(3,1));
 B(4,1) = fzero(f,12); B(4,2)=tan(B(4,1))-tanh(B(4,1));
 B(5,1) = fzero(f,15); B(5,2)=tan(B(5,1))-tanh(B(5,1));
 B(6,1) = fzero(f,18); B(6,2)=tan(B(6,1))-tanh(B(6,1));
 B;
BETA=B(:,1)/l; % [1/ft]

% ------------------------------- ROOT 1 ------------------------------
- %
 BB=B(1,1)/l;

CONST(1) =(sin(BB*l)+sinh(BB*l))/(cos(BB*l)-cosh(BB*l)) % [ft]/[ft] ok
Q = quad(' (cos(x) - cosh(x) - 0.9825*( sin(x)-
sinh(x))).^2',0,l) %BB*l     % [ft]
```

```
C4(1) = sqrt(1/(Q*12*p*A)); % conversion from FT to IN ; C4 = sqrt(1/M)
Wn = C4(1) * 12*( (cos(BB*x)-cosh(BB*x)) + CONST(1)*( sin(BB*x)-
sinh(BB.*x)) ); % [IN./M]


figure(1)
subplot(1,4,1)
plot( Wn ,x)
% ------------------------------- ROOT 2 ------------------------------
- %
 BB=B(2,1)/l;

CONST(2) =(sin(BB*l)+sinh(BB*l))/(cos(BB*l)-cosh(BB*l))
Q = quad(' (cos(x) - cosh(x) - 1.0*( sin(x) - sinh(x))).^2',0,l) %BB*l
C4(2) = sqrt(1/(Q*12 *p*A));
Wn = C4(2) * 12*( (cos(BB*x)-cosh(BB*x)) + CONST(2)*( sin(BB*x)-
sinh(BB.*x)) );

figure(1)
subplot(1,4,2)
plot( Wn ,x)
% ------------------------------- ROOT 3 ------------------------------
- %
 BB=B(3,1)/l;

 CONST(3) =(sin(BB*l)+sinh(BB*l))/(cos(BB*l)-cosh(BB*l));

Q = quad(' (cos(x) - cosh(x) - 1.0*( sin(x) - sinh(x))).^2',0,l) %BB*l
C4(3) = sqrt(1/(Q*12 *p*A));
Wn = C4(3) * 12*( (cos(BB*x)-cosh(BB*x)) + CONST(3)*( sin(BB*x)-
sinh(BB.*x)) );

figure(1)
subplot(1,4,3)
plot( Wn ,x)
% ------------------------------- ROOT 4 ------------------------------
- %
 BB=B(4,1)/l;

CONST(4) =(sin(BB*l)+sinh(BB*l))/(cos(BB*l)-cosh(BB*l));
Q = quad(' (cos(x) - cosh(x) - 1.0*( sin(x) - sinh(x))).^2',0,l) %BB*l
C4(4) = sqrt(1/(Q*12 *p*A))
Wn = C4(4) * 12*( (cos(BB*x)-cosh(BB*x)) + CONST(4)*( sin(BB*x)-
sinh(BB.*x)) );

figure(1)
subplot(1,4,4)
plot( Wn ,x)

% ------------------------ PLOT SETTINGS ------------------------ %
subplot(1,4,1)
title('\bf\beta_1l=2.3650')
```

```
xlabel('\bfW_n(in.)');ylabel('\bfColumn Height(ft.)')
subplot(1,4,2)
title('\bf\beta_2l=5.4978')
xlabel('\bfW_n(in.)');
subplot(1,4,3)
title('\bf\beta_3l=8.6394')
xlabel('\bfW_n(in.)');
subplot(1,4,4)
title('\bf\beta_4l=11.7810')
xlabel('\bfW_n(in.)');
```

LocMaxCurv.m

This user defined function locates the maximum curvature using the derivatives of the transient equation. The sign of the fourth derivative allows for a manual check.

```
function [ModVal] = LocMaxCurv(x,root_num)

global BETA l p A CONST C4

% This function will find the W(x) value for the location of the max
% curvature
%
% root / B = l = x
% x = location (length) [ft]
%
% matrix ModVal includes the following
%       Col 1: W(x)
%       Col 2: W'(x)
%       Col 3: W''(x)
%       Col 4: W'''(x)
%       Col 5: W''''(x)

z=length(x); %[ft]
C4n = C4(root_num); % slugs^ -.5 *** should be unitless
K = CONST(root_num); % unitless
B = BETA(root_num); % [1/ft]?


ModVal(1:z,1)     = (C4n * B^0) .*( (cos(B.*x) - cosh(B.*x) ) + ...
             K .* (sin(B.*x) - sinh(B.*x)) );
ModVal(1:z,2)     = (C4n * B^1) .*( (-sin(B.*x) - sinh(B.*x) ) + ...
             K .* (cos(B.*x) - cosh(B.*x)) );
ModVal(1:z,3)    = (C4n * B^2) .*( (-cos(B.*x) - cosh(B.*x) ) + ...
             K .* (-sin(B.*x) - sinh(B.*x)) );
ModVal(1:z,4)   = (C4n * B^3) .*( ( sin(B.*x) - sinh(B.*x) ) + ...
             K .* (-cos(B.*x) - cosh(B.*x)) );
ModVal(1:z,5) = (C4n * B^4) .*( ( cos(B.*x) - cosh(B.*x) ) + ...
             K .* (sin(B.*x) - sinh(B.*x)) );
```

A.4.4 MaxCurvature.m

This user defined function finds the maximum curvature location.

```
function [] = MaxCurvature ()
%*********************************************************************
*
%***************  Function MaxCurvature ****************************
%*********************************************************************
*
%
%                 Undergraduate Research Scholars
% ************************************************************
% This function calculates for the maximum curvature of the
% mode shape equation W(x).
%
%
% ----------------  ** Useful defined Equations ** ----------------
%
%  (1)   W_n(x)  =  C_4n * ( cos Bx - cosh Bx ) + Kn * ( sin Bx - sinh
Bx )
%  (2)     Kn    =  ( sin B*l + sinh B*l ) / ( cos Bl - cosh Bl )
%  (3) W_n'''(x) =  C_4n * B^3 * ( sin Bx - sinh Bx ) - ...
%                       Kn* ( cos Bx + cosh Bx )
%  (4) W_n''''(x) =  C_4n * B^4 * ( cos Bx - cosh Bx ) + ...
%                       Kn* ( sin Bx - sinh Bx )
%
% ---------------- ---------------- ---------------- ----------------
%
% Roldan, Alejandra L.
% Modified last: 3/23/11
%
clc;clear;

global BETA l p A CONST C4 Wn ModVal1

% %....... Begin Code Block 1
% ModeFinding;
% %....... End of Code Block 1


% ................. Begin Code Block 2: Root 1
K = CONST(1)
B = BETA(1); % 1/ft.
C4n = C4(1) % slugs^ -.5**

f = @(y) (sin(y)-sinh(y))/((cos(y)+cosh(y)))-K;
y(1) = fzero(f,3); % 2.3650 BL
x = y./B; % length (ft.)

% Location of max curv
ModVal1 = LocMaxCurv(x,1)
```

```
% Check by Plot
z=0:0.01:1;
W1    = (C4n * B^0) .*( (cos(B.*z) - cosh(B.*z) ) + ...
             K .* (sin(B.*z) - sinh(B.*z)) );
dW1   = (C4n * B^1) .*( (-sin(B.*z) - sinh(B.*z) ) + ...
             K .* (cos(B.*z) - cosh(B.*z)) );
ddW1  = (C4n * B^2) .*( (-cos(B.*z) - cosh(B.*z) ) + ...
             K .* (-sin(B.*z) - sinh(B.*z)) );
dddW1 = (C4n * B^3) .*( ( sin(B.*z) - sinh(B.*z) ) + ...
             K .* (-cos(B.*z) - cosh(B.*z)) );
ddddW1= (C4n * B^4) .*( ( cos(B.*z) - cosh(B.*z) ) + ...
             K .* (sin(B.*z) - sinh(B.*z)) );
figure(2)
subplot(1,5,1)
plot(W1,z);hold on;plot(ModVal1(:,1),x,'ro')
subplot(1,5,2)
plot(dW1,z);hold on;plot(ModVal1(:,2),x,'ro')
subplot(1,5,3)
plot(ddW1,z);hold on;plot(ModVal1(:,3),x,'ro')
subplot(1,5,4)
plot(dddW1,z);hold on;plot(ModVal1(:,4),x,'ro')
subplot(1,5,5);hold on;plot(ModVal1(:,5),x,'ro')
plot(ddddW1,z)

% plot settings
subplot(1,5,1); title('\bfW_1')
subplot(1,5,2); title('\bfdW_1')
subplot(1,5,3); title('\bfddW_1')
subplot(1,5,4); title('\bfdddW_1')
subplot(1,5,5); title('\bfddddW_1')

% ................. End Code Block 2: Root 1



% ................. Begin Code Block 2: Root 2
K = CONST(2);
B = BETA(2);
C4n = C4(2);

f = @(y) (sin(y)-sinh(y))/((cos(y)+cosh(y)))-K;
y(1) = fzero(f,3); % 2.4191
y(2) = fzero(f,5); % 5.4978
x = y./B;

% Location of max curv
ModVal2 = LocMaxCurv(x,2)

% Check by Plot
z=0:0.01:1;
W2    = (C4n * B^0) .*( (cos(B.*z) - cosh(B.*z) ) + ...
```

```
             K .* (sin(B.*z) - sinh(B.*z)) );
dW2   = (C4n * B^1) .*( (-sin(B.*z) - sinh(B.*z) ) + ...
             K .* (cos(B.*z) - cosh(B.*z)) );
ddW2  = (C4n * B^2) .*( (-cos(B.*z) - cosh(B.*z) ) + ...
             K .* (-sin(B.*z) - sinh(B.*z)) );
dddW2 = (C4n * B^3) .*( ( sin(B.*z) - sinh(B.*z) ) + ...
             K .* (-cos(B.*z) - cosh(B.*z)) );
ddddW2= (C4n * B^4) .*( ( cos(B.*z) - cosh(B.*z) ) + ...
             K .* (sin(B.*z) - sinh(B.*z)) );
figure(3)
subplot(1,5,1)
plot(W2,z);hold on;plot(ModVal2(:,1),x,'ro')
subplot(1,5,2)
plot(dW2,z);hold on;plot(ModVal2(:,2),x,'ro')
subplot(1,5,3)
plot(ddW2,z);hold on;plot(ModVal2(:,3),x,'ro')
subplot(1,5,4)
plot(dddW2,z);hold on;plot(ModVal2(:,4),x,'ro')
subplot(1,5,5);hold on;plot(ModVal2(:,5),x,'ro')
plot(ddddW2,z)

% plot settings
subplot(1,5,1); title('\bfW_2')
subplot(1,5,2); title('\bfdW_2')
subplot(1,5,3); title('\bfddW_2')
subplot(1,5,4); title('\bfdddW_2')
subplot(1,5,5); title('\bfddddW_2')

% ................. End Code Block 2: Root 2


% ................. Begin Code Block 2: Root 3
K=CONST(3);
B = BETA(3); % already dependent on defined LENGTH

f = @(y) (sin(y)-sinh(y))/((cos(y)+cosh(y)))-K;
y(1) = fzero(f,2); % 2.4192
y(2) = fzero(f,5); % 5.4949
y(3) = fzero(f,8); % 8.6394
x = y./B;
% Location of max curv
ModVal3 = LocMaxCurv(x,3)

% Check by Plot
z=0:0.01:1;
W3    = (C4n * B^0) .*( (cos(B.*z) - cosh(B.*z) ) + ...
             K .* (sin(B.*z) - sinh(B.*z)) );
dW3   = (C4n * B^1) .*( (-sin(B.*z) - sinh(B.*z) ) + ...
             K .* (cos(B.*z) - cosh(B.*z)) );
ddW3  = (C4n * B^2) .*( (-cos(B.*z) - cosh(B.*z) ) + ...
             K .* (-sin(B.*z) - sinh(B.*z)) );
dddW3 = (C4n * B^3) .*( ( sin(B.*z) - sinh(B.*z) ) + ...
             K .* (-cos(B.*z) - cosh(B.*z)) );
```

```
ddddW3= (C4n * B^4) .*( ( cos(B.*z) - cosh(B.*z) ) + ...
             K .* (sin(B.*z) - sinh(B.*z)) );
figure(4)
subplot(1,5,1)
plot(W3,z);hold on;plot(ModVal3(:,1),x,'ro')
subplot(1,5,2)
plot(dW3,z);hold on;plot(ModVal3(:,2),x,'ro')
subplot(1,5,3)
plot(ddW3,z);hold on;plot(ModVal3(:,3),x,'ro')
subplot(1,5,4)
plot(dddW3,z);hold on;plot(ModVal3(:,4),x,'ro')
subplot(1,5,5);hold on;plot(ModVal3(:,5),x,'ro')
plot(ddddW3,z)

% plot settings
subplot(1,5,1); title('\bfW_3')
subplot(1,5,2); title('\bfdW_3')
subplot(1,5,3); title('\bfddW_3')
subplot(1,5,4); title('\bfdddW_3')
subplot(1,5,5); title('\bfddddW_3')
% ................. End Code Block 2: Root 3



% ................. Begin Code Block 2: Root 4
K=CONST(4);
B = BETA(4);
C4n = C4(4);

f = @(y) (sin(y)-sinh(y))/((cos(y)+cosh(y)))-K;
y(1) = fzero(f,2);   % 2.4192
y(2) = fzero(f,6);   % 5.4949
y(3) = fzero(f,8);   % 8.6395
y(4) = fzero(f,11);  % % 11.7810
x = y./B;
% Location of max curv
ModVal4 = LocMaxCurv(x,4)

% Check by Plot
z=0:0.01:1;
W4    = (C4n * B^0) .*( (cos(B.*z) - cosh(B.*z) ) + ...
             K .* (sin(B.*z) - sinh(B.*z)) );
dW4   = (C4n * B^1) .*( (-sin(B.*z) - sinh(B.*z) ) + ...
             K .* (cos(B.*z) - cosh(B.*z)) );
ddW4  = (C4n * B^2) .*( (-cos(B.*z) - cosh(B.*z) ) + ...
             K .* (-sin(B.*z) - sinh(B.*z)) );
dddW4 = (C4n * B^3) .*( ( sin(B.*z) - sinh(B.*z) ) + ...
             K .* (-cos(B.*z) - cosh(B.*z)) );
ddddW4= (C4n * B^4) .*( ( cos(B.*z) - cosh(B.*z) ) + ...
             K .* (sin(B.*z) - sinh(B.*z)) );
figure(5)
subplot(1,5,1)
plot(W4,z);hold on;plot(ModVal4(:,1),x,'ro')
```

```
subplot(1,5,2)
plot(dW4,z);hold on;plot(ModVal4(:,2),x,'ro')
subplot(1,5,3)
plot(ddW4,z);hold on;plot(ModVal4(:,3),x,'ro')
subplot(1,5,4)
plot(dddW4,z);hold on;plot(ModVal4(:,4),x,'ro')
subplot(1,5,5);hold on;plot(ModVal4(:,5),x,'ro')
plot(ddddW4,z)

% plot settings
subplot(1,5,1); title('\bfW_4')
subplot(1,5,2); title('\bfdW_4')
subplot(1,5,3); title('\bfddW_4')
subplot(1,5,4); title('\bfdddW_4')
subplot(1,5,5); title('\bfddddW_4')
% ................. End Code Block 2: Root 4
```

CONTACT INFORMATION

Name:	Alejandra Lucia Roldan Arcos
Professional Address:	c/o Dr. Luciana Barroso Department of Civil Engineering CE/TTI 705J Texas A&M University College Station, TX 77843
Email Address:	aleroldan12@gmail.com
Education:	B.S. Civil Engineering Texas A&M University, Dec. 2011 Undergraduate Research Scholar